A Deep Space Orbit Determination Software: Overview and Event Prediction Capability

Youngkwang Kim, Sang-Young Park[†], Eunji Lee, Minsik Kim
Department of Astronomy, Yonsei University, Seoul 03722, Korea

This paper presents an overview of deep space orbit determination software (DSODS), as well as validation and verification results on its event prediction capabilities. DSODS was developed in the MATLAB object-oriented programming environment to support the Korea Pathfinder Lunar Orbiter (KPLO) mission. DSODS has three major capabilities: celestial event prediction for spacecraft, orbit determination with deep space network (DSN) tracking data, and DSN tracking data simulation. To achieve its functionality requirements, DSODS consists of four modules: orbit propagation (OP), event prediction (EP), data simulation (DS), and orbit determination (OD) modules. This paper explains the highest-level data flows between modules in event prediction, orbit determination, and tracking data simulation processes. Furthermore, to address the event prediction capability of DSODS, this paper introduces OP and EP modules. The role of the OP module is to handle time and coordinate system conversions, to propagate spacecraft trajectories, and to handle the ephemerides of spacecraft and celestial bodies. Currently, the OP module utilizes the General Mission Analysis Tool (GMAT) as a third-party software component for high-fidelity deep space propagation, as well as time and coordinate system conversions. The role of the EP module is to predict celestial events, including eclipses, and ground station visibilities, and this paper presents the functionality requirements of the EP module. The validation and verification results show that, for most cases, event prediction errors were less than 10 millisec when compared with flight proven mission analysis tools such as GMAT and Systems Tool Kit (STK). Thus, we conclude that DSODS is capable of predicting events for the KPLO in real mission applications.

Keywords: deep space navigation, Korea pathfinder lunar orbiter, event prediction

1. INTRODUCTION

For deep space exploration, deep space navigation techniques are essential. The deep space navigation process includes three major components: tracking spacecraft, orbit determination, and guidance operation. To track spacecraft in deep space, ground-based radiometric and onboard optical measurements are typically used. The deep space network (DSN) is the best-known ground station network providing radiometric tracking services. Onboard optical measurements may or may not be used for deep space navigation, depending on mission requirements. For instance, the Mars Pathfinder, Mars Climate Orbiter, and Mars Polar Lander only used radiometric tracking data for deep space navigation (Thornton & Border 2003). Orbit determination is a process for estimating

the previous or current orbital state and spacecraft properties using tracking data. Based on the orbit determination results, guidance operations are applied to spacecraft to maintain or achieve the desired trajectory.

There have been efforts to develop deep space navigation software to support deep space missions using ground-based radiometric spacecraft tracking. Although government space agencies capable of deep space missions may have their own in-house deep space navigation software packages, there are few deep space navigation software packages available or purchasable for the general public. General Mission Analysis Tool (GMAT) is an open-source software package developed by the Goddard Space Flight Center (GSFC) and collaborators, and GMAT has an external navigation plugin including the DSN two-way range, Doppler observation

models, and a batch least squares estimator (Hughes et al. 2017). The GSFC is planning to replace the legacy software package GTDS with GMAT, and the first target is to operate the SOHO mission with GMAT in the near future (Hughes et al. 2017). MONTE is a commercial software package developed by the Jet Propulsion Laboratory (JPL). MONTE is based on the JPL's legacy software packages DPTRAJ and ODP, and has served all of JPL's deep space missions, such as Cassini and Gravity Recovery And Interior Laboratory (GRAIL), since 2012 (JPL 2017). The orbit determination tool kit (OTDK) is a commercial software package developed by Analytical Graphics Inc., and has been successfully applied to the Lunar Atmosphere and Dust Environment Explorer (LADEE) mission along with the company's other software package, Systems Tool Kit (STK) (D'Ortenzio et al. 2015).

There are pros and cons of using commercial or open-source deep space navigation software to support a deep space mission. Using commercial or open-source deep space navigation software can save time and efforts compared to developing and maintaining mission-specific deep space navigation software. Sometimes, using external navigation software can be cost-effective compared to developing mission-specific navigation software when there is no legacy software to refer to for the development. Conversely, the usage of commercial or open-source deep space navigation software is not always acceptable, depending on mission requirements and specifications. For instance, the current version of GMAT does not support prediction of solar outage but predicting solar outage may provide necessary support to a deep space mission in certain situations. In addition, the specific software input and/or output interface may differ from desirable interface specifications. Thus, using commercial or open-source deep space navigation software can be a good option, if the mission requirements and interface specifications are well supported by affordable software packages. However, where this is not the case, it is necessary to develop mission-specific deep space navigation software.

This paper introduces deep space orbit determination software (DSODS), which is a Mathwork's MATLAB object-oriented programming environment-based navigation software for deep space missions developed by Yonsei University in collaboration with the Korean Aerospace Research Institute (KARI) to support the Korea Pathfinder Lunar Orbiter (KPLO) mission. DSODS has three major capabilities: celestial event prediction for spacecraft, orbit determination with DSN tracking data, and DSN tracking data simulation. DSODS satisfies the current functionality requirements of the KPLO mission regarding orbit determination, data simulation, and event prediction, and will support the related interface specifications for the KPLO. This paper addresses only the validation

and verification of event prediction capability. Its orbit determination and tracking data simulation capabilities are validated and verified for lunar missions based on processing and analysis of the flight data of Lunar Prospector, which was one of the National Aeronautics and Space Administration (NASA) Discovery missions (Kim et al. 2017a, b; Lee et al. 2017).

There are two goals of this paper: introducing an overview of DSODS and addressing event prediction capabilities in terms of how they work and their validation and verification. Three main drivers affected the overall design of the DSODS: compatibility with GMAT, the interfaces between modules, and the input and output data specifications. The compatibility with GMAT was important because the orbit propagation (OP) module now utilizes GMAT as a third-party software component, and GMAT has been in charge of handling fundamental astrodynamics-related operations. This decision has significantly shortened the overall development period of DSODS, and minimized the efforts spent on the development and testing of the OP module. However, a drawback of using large third-party software such as GMAT is that the limitations of GMAT are the same as those of DSODS. For instance, currently, GMAT and DSODS only support gravitational potential data with a degree and order equal to or less than 165. To mitigate such limitations, all GMAT dependent components are located in the OP module and isolated from event prediction (EP), data simulation (DS), and orbit determination (OD) modules. Thus, only the OP module needs to be modified to replace GMAT with another third-party software, if necessary.

The EP module determines the locations of events in the time domain based on a geometrical approach (Parker & Hughes 2011). Currently, the EP module satisfies the functionality requirements of the KPLO (Song et al. 2016), and is expected to satisfy the future performance requirements of the KPLO. The EP module consists of three major components: event functions, an analytical event location algorithm, and a mesh-refinement algorithm. An event function is defined as when a corresponding type of event (e.g., eclipse) occurs, the value of the event function is always equal to zero. From such a definition, it is clear that finding the roots of the event function is equivalent to locating the event. To find the roots of the event function, the analytical event location algorithm utilizes a cubic Hermite spline and analytical roots of the cubic equation. The merit of the analytical event location algorithm is that it does not require an iterative process to locate the roots. For accuracy control of the event prediction results, a mesh-refinement algorithm is applied to the EP module because event prediction accuracy is dependent on the event function data-sampling rate. The mesh-refinement algorithm estimates the relative errors

between the event prediction solutions from two different sampling rates, and applies increased sampling rates in the intervals where the relative errors do not satisfy the user-defined tolerance. To validate and verify the event prediction capabilities of DSODS, a carefully selected set of test problems is implemented according to the functionality requirements, and the external truth data are generated using flight-proven software packages such as Spacecraft Planet Instrument C-matrix Events (SPICE), STK, and GMAT.

In Section 2, a brief explanation of the Common Utility and Class Library (CUCL) and the highest-level data flows for event prediction, orbit determination, and tracking data simulation are presented. Sections 3 and 4 address OP and EP modules in light of their responsibilities and how they work, respectively. In addition, Section 4 includes the validation and verification results on the DSODS event prediction capabilities. In Section 5, the summary and conclusions of this study are presented.

2. DSODS OVERVIEW

This section presents an overview on some important features of DSODS including the user environment, CUCL, and representative examples on its major applications with key data flows. Now, DSODS supports a script-based user interface, and is executable with a MATLAB 32-bit version higher than 2013b under Microsoft's Windows OS environment. Such limitations exist for two reasons. First, DSODS was developed based on MATLAB object-oriented programming, and the MATLAB object-oriented programming environment is rapidly changing due to its active development. Second, DSODS includes some 32-bit MATLAB executable files to improve execution speed, and to interface GMAT because GMAT is a 32-bit application mainly written in C++ with some legacy FORTRAN components. Note that GMAT has been used for fundamental astrodynamics-related operations as a third-party component. The details of the MATLAB-executable (MEX) based GMAT interface is introduced in Section 3.

DSODS consists of one library named CUCL, and four modules: OP, EP, DS, and OD modules. The CUCL includes common utilities and fundamental classes used by multiple modules such as the epoch time, coordinate, ephemeris, spacecraft, and ground station classes, etc. The OP module is responsible for fundamental astrodynamics operations such as time and coordinate system conversions, orbit propagation of spacecraft orbit, and providing ephemerides of celestial bodies. The EP module is responsible for predicting celestial events such as eclipses, apsis passages, node crossings, solar

communication interferences, and ground station visibilities. The DS and OD modules are closely tied, and responsible for orbit determination of spacecraft and tracking data simulation. The DS module includes the DSN sequential range and Doppler observation models, their noise characteristics, and media and antenna correction models. Using the DS module, the OD module conducts orbit determination with DSN tracking data files written in tracking data message (TDM) format, which is an international tracking data format standard defined by the Consultative Committee For Space Data Systems (CCSDS). The OD module generates pseudo DSN tracking data written in the TDM format. In the OD module, a batch least squares estimation algorithm has been implemented to solve the orbit determination problem (Cappellari et al. 1976). In addition, the OD module provides covariance analysis methods such as covariance propagation, projection, and transformation.

Fig. 1(a) shows the highest-level data flow of the DSODS event prediction process. The user or OD module can make an event prediction request for the EP module with the spacecraft ephemeris, ground station list, and/or list of occulting bodies (i.e., the Moon), as well as relevant settings. To generate the spacecraft ephemeris, it is possible to utilize the OP module, but the EP module cannot distinguish whether the spacecraft ephemeris is generated by the OP module or other tools such as STK and GMAT, as long as the ephemeris is written in STK's ephemeris or CCSDS OEM format. If needed, the EP module obtains ground station (GS) and/or celestial body (CB) ephemerides using the OP module. Using the ephemerides of spacecraft (SC), GS, and/or CB, the EP module locates the desired events in the time domains, and delivers the event prediction results to the user or OD module. There are two possible forms of event prediction results: a text-based event prediction report and instances of Event Prediction class, which are discussed in Section 4.

Fig. 1(b) shows the highest-level data flow of the DSODS orbit determination process. The user can make an orbit determination request from the OD module with an initial guess on solve-for parameters (e.g. the initial state vector of the spacecraft, the spacecraft solar radiation pressure (SRP) area, and range/Doppler biases), spacecraft, spacecraft tracking data in CCSDS TDM format, and relevant settings. Based on the user's input data, the OD module conducts orbit determination with a weighted batch least squares estimation algorithm (Cappellari et al. 1976). Tracking data includes information on the ground station, DSN measurement settings for range and Doppler observables, DSN measurements, and time tags of measurements. Note that all the range and Doppler observations include radio signal integration over the time interval, and a time
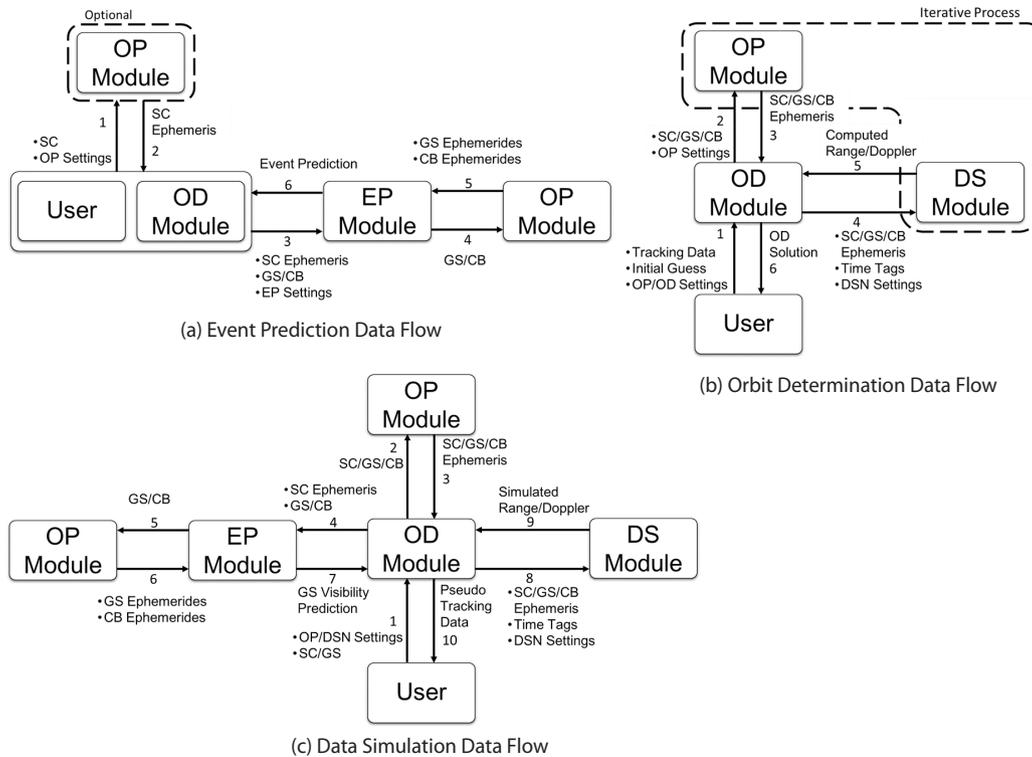
Fig. 1. Data flow diagrams for: (a) event prediction, (b) orbit determination, and (c) data simulation.

tag represents the measurement time. The OD module obtains ephemerides of the spacecraft, ground stations, and celestial bodies using the OP module with the spacecraft, ground stations, and relevant settings. Then, the OD module acquires the computed range and Doppler observables using the DS module with the ephemerides and relevant settings. The OD module then calculates the residuals between the computed and observed DSN measurements so that the OD module updates solve-for parameters to reduce the weighted least squares of residuals. If solve-for parameters are converged, the OD module delivers the orbit determination solution to the user. Otherwise, the OD module continues updating solve-for parameters until solve-for parameters converge or the number of iterations reaches the predefined maximum iteration number. As a result, the OD module produces a readable report in the DSODS format. The OD report includes information on the solve-for parameter solution, the covariance of the OD solution, measurement residuals, the measurement data editing history, DSN settings, and orbit propagation settings.

Fig. 1(c) shows the highest-level data flow of the DSODS tracking data simulation process. The user can make a DSN measurement data simulation request to the OD module with the truth data for solve-for parameters (e.g. initial state vector of spacecraft, spacecraft SRP area, and range/Doppler biases), spacecraft, ground stations, and relevant settings.

Using the DS and EP modules, the OD module creates a set of simulated range and/or Doppler measurements, and saves it in a text file written in the CCSDS TDM format. Compared to event prediction and orbit determination processes, the tracking data simulation process includes the majority of event prediction and orbit determination processes, except the iterative process. In addition, in the tracking data simulation process, the DS module does not produce computed range and Doppler observables but simulated sequential range and Doppler observables, which include simulated white noise and user-defined biases.

2.1 CUCL

This subsection explains some important concepts including time and ephemeris, and how they are handled in DSODS with the CUCL. Now, the CUCL consists of six important classes and utility subroutines: epoch time, coordinate system base, Hermite ephemeris, spacecraft, transponder, and ground station base. Among them, epoch time, coordinate system base, and spacecraft are associated with GMAT and compatible with the GMAT corresponding counterpart classes. The utility subroutines are not directly addressed here because there are a number of subroutines in DSODS. Thus, the following explanation on CUCL focuses on the classes in terms of information and functionalities.

The CUCL was developed to efficiently handle the interfaces between modules and various input and output data specifications. The CUCL includes a number of utility subroutines and six classes used throughout the DSODS. For instance, the epoch time class of the CUCL supports five time system types, which are international atomic time (TAI), terrestrial time (TT), barycentric dynamical time (TDB), coordinated universal time (UTC), and A1 (U.S. Naval Observatory's atomic time scale; a predecessor of TAI), and four time representations (i.e., GMAT style modified Julian Date, numerical Gregorian, GMAT style Gregorian string, and CCSDS style Gregorian string). Note that handling epochs given in various representation types is important to support general input and output specifications such as the CCSDS orbit ephemeris message (OEM) format, which is an international orbit data format standard defined by CCSDS, and STK's own ephemeris format.

Time is one of the most fundamental concepts in astrodynamics, and needs to be handled with discretion. Currently, the epoch time class contains information on the epoch time, its time system type (e.g. TAI), and its representation type, for instance, Gregorian or modified Julian date (MJD). In addition, epoch time provides functionalities such as conversions between representation types and calculation of the elapsed seconds between different epochs. The epoch time class supports five time system types: TAI, TT, TDB, UTC, and A1. Inside DSODS, any time moment is defined in terms of the epoch time t_0^{SYS}, TAI elapsed seconds Δt^{TAI}, and time rate correction (Δt^{SYS}-Δt^{TAI}), as follows:

$$t^{\text{SYS}} = t_0^{\text{SYS}} + \Delta t^{\text{TAI}} + \left(\Delta t^{\text{SYS}} - \Delta t^{\text{TAI}}\right) \tag{1}$$

where the superscript SYS represents the time system type. Regarding the time rate correction term, the following holds:

$$\Delta t^{\text{UTC}} = \Delta t^{\text{TAI}} = \Delta t^{\text{TT}} = \Delta t^{\text{A1}} \neq \Delta t^{\text{TDB}} \tag{2}$$

Thus, the time rate correction term is not equal to zero only for the TDB time system. Note that one second in TDB is different from one second of the other time systems due to the general relativistic time dilation effect (Moyer 2005). The time rate correction for TDB is realized in the DS module for the general relativistic light propagation in the solar system barycentric space-time reference system. Moreover, the time difference $\Delta t_{\text{B}}^{\text{A}}$ between the time values in two different time systems is defined as follows:

$$t^{\text{A}} = t^{\text{B}} + \Delta t_{\text{B}}^{\text{A}} \tag{3}$$

where A and B are one of any time system supported in DSODS. Both the time rate corrections and time difference

is now handled by GMAT. In the near future, DSODS will replace GMAT-related time conversion algorithms with its own time conversion algorithms. On the other hand, the epoch time class supports fours time representations: the GMAT style modified Julian Date, numerical Gregorian, the GMAT style Gregorian string, and the CCSDS style Gregorian string. Gregorian representation expresses a time moment by year, month, day, hour, minute, and second. Supporting various time representations is important for generalizing input and output specifications because each specification uses a different representation. For instance, TDM, and OEM formats are based on the CCSDS style Gregorian (e.g. 2000-01-01T12:00:00.000), whereas STK and GMAT time representations are based on the GMAT style Gregorian (e.g. 01 Jan 2000 12:00:00.000). Additionally, the usual MJD offset from Julian date (JD) is defined as 2400000.5 but DSODS uses the GMAT style modified Julian date, which is defined as:

$$t_{\text{MJD}} = t_{\text{JD}} - 2430000.0 \tag{4}$$

where 2430000.0 is the GMAT's MJD offset from JD. The conversion between MJD and Gregorian representations can cause numerical noise associated with dividing by 86,400 (a day in seconds). To suppress such numerical noise, DSODS supports setting the time resolution for conversion. For instance, if the user set the time resolution to be 10^{-6}, DSODS rounds a second of the Gregorian representation with respect to six digits to the right of the decimal point. The default time resolution is set as 10^{-6} in DSODS.

In DSODS, the coordinate system base class allows the user to define various coordinate systems as a combination of the reference points and axis type. The coordinate system base class is responsible for reproducing GMAT coordinate systems through the GMAT interface. As a result, the conversions between different coordinate systems are handled entirely by GMAT. In accordance with GMAT, the coordinate system base class supports six axis types: J2000 equatorial, J2000 ecliptic, ICRF, object referenced, body fixed, and body inertial, and supports three types of coordinate system references: celestial point, spacecraft, and ground station. For celestial points, there are ten supported references: solar system barycenter, Sun, Mercury, Venus, Earth, Luna, Mars, Jupiter, Saturn, Uranus, Neptune, and Pluto. Apart from the object reference axis type, the coordinate system has only one reference point that is the center of the coordinate. The object reference axis type constructs a local-vertical-local-horizontal (LVLH) axis, where the radial direction is defined by the vector from the first reference to the second reference, the normal direction is defined by the angular momentum vector, and the other direction is co-normal to the radial and normal

directions. The center of the coordinate is defined as the second reference point. Therefore, DSODS allows the user to define a variety of coordinate systems as a combination of the reference points and the axis type. For more details, see the GMAT mathematical specification document (GMAT 2017).

Inside of DSODS, the Hermite ephemeris class is used to define any ephemeris as a set of polynomial coefficients to interpolate position and velocity vectors at any moment within the predefined interval by Hermite interpolation. Hermite interpolation guarantees consistency between position and velocity interpolations, which means that the derivative of the polynomial interpolating position is equal to the polynomial interpolating velocity (Zill et al. 2011). Although the concept of ephemeris is originally defined for a space object such as a celestial body or spacecraft, the Hermite ephemeris class of DSODS supports any object, including a ground station, with a position and velocity as a function of time within the predefined interval. The extended concept of ephemeris is used throughout DSODS, and is especially useful for handling iterative processes, such as root-finding in the EP module and light time equation solving in the DS module, because these iterative processes requires the position and velocity of an object as continuous curves rather than a set of discrete points. Currently, the Hermite ephemeris class uses polynomials of the fifth degree for each coordinate by default, and allows the user to use polynomials ranging from the third to the seventh degree.

Similar to the coordinate system base class, the spacecraft class of DSODS is responsible for reproducing GMAT spacecraft through the GMAT interface. The spacecraft class contains information on the name, epoch time, initial state vector, coordinate system, representation type, drag area and coefficient, SRP area and reflectivity, and transponder of a spacecraft. It supports three state representation types: Cartesian, classical Keplerian, and spherical coordinate state representation based on right ascension and declination. Moreover, a transponder is represented as a class in DSODS, which contains information on the uplink and downlink bands, turn around ratio, and transponder delay in meters. In the DSN sequential range observable, transponder delay plays an important role because its magnitude is usually several hundred meters, e.g., the Lunar Prospector transponder delay was measured as 405 m (Woodburn & Seago 2008).

The ground station base class of the CUCL plays an important role in DSODS. The ground station base class contains information on the location, range and Doppler biases, range and Doppler noise levels, antenna related information (such as cut off angle for contact, diameter, antenna offset constant, and mount type), and mean meteorological models (ODTBX 2017) for DSN complexes. Also, the ground station base class provides the methods for conversions between Cartesian and geodetic spherical coordinates, antenna offset correction calculations, and media correction calculations based on mean meteorological models.

3. OP MODULE

The OP module is responsible for fundamental astrodynamics-related operations: orbit propagation, time and coordinate system conversions, and creation of spacecraft and celestial body ephemerides. Currently, the OP module utilizes the GMAT as a third-party software component, and the GMAT is in charge of handling these fundamental operations. For mathematical details, see the GMAT mathematical specification document (GMAT 2017). Although using the GMAT has significantly shortened the overall development period of DSODS, the capability and application environment of the OP module is limited by the GMAT. For instance, currently, the GMAT supports only gravitational potential data with a degree and order equal to or less than 165. In addition, the user needs a MATLAB 32-bit version higher than 2013b to run DSODS under the Microsoft Windows OS environment. However, the OP module includes all the GMAT dependent codes so that the other modules cannot distinguish whether the OP module is using the GMAT or not. Such GMAT dependency isolation was intended to make the GMAT replaceable with other third-party software in the future.

The OP module consists of module-level methods, the MATLAB/GMAT interface, and public classes. Table 1 explains the module-level methods provided by the OP module. These module-level methods are used by the other modules throughout DSODS. Table 2 introduces the components of the MATLAB/GMAT interface with brief explanations. There are six components: script interface,

Table 1. OP module method list

Method Name	Role
Time Conversion Utility	To convert time systems between UTC, TAI, TT, A1, and TDB
Coordinate Conversion Utility	To convert coordinate systems between any types supported in DSODS
Propagate SC	To propagate spacecraft trajectory with gravitational potential, air-drag, SRP, third body, and relativistic effects
Get GS State Array	To convert ECEF coordinates to ECI coordinates based on IAU-1976 and FK5 theory with 1980 update to nutation
Get CB State Array	To calculate celestial bodies' state vectors based on JPL's DE421 ephemeris data

Table 2. MATLAB/GMAT interface component list

Name	Type	Explanation
Script Interface	MATLAB class	Script interface is responsible for generating GMAT script for orbit propagation using Force Model, Propagator, and Spacecraft classes.
Class Interface	MATLAB class	Class interface owns MEX interface. Its role is to interface MEX interface and OP module methods.
MEX Interface	32-bit MEX	MEX interface utilizes GMAT interface. Its role is to deliver data from OP module to GMAT and vice versa.
GMAT Interface	C++ class	GMAT interface is a part of MEX interface, and knows the details of GMAT classes. Its role is to obtain the desired data using GMAT.
libGmatBase	32-bit DLL	libGmatBase is the GMAT base library. Its role is to conduct fundamental astrodynamics-related operations.
GMAT Data	text and binary	The various text and binary data included in GMAT. They are required to conduct fundamental astrodynamics-related operations.

(a) OP Module Data Flow Type A   (b) OP Module Data Flow Type B
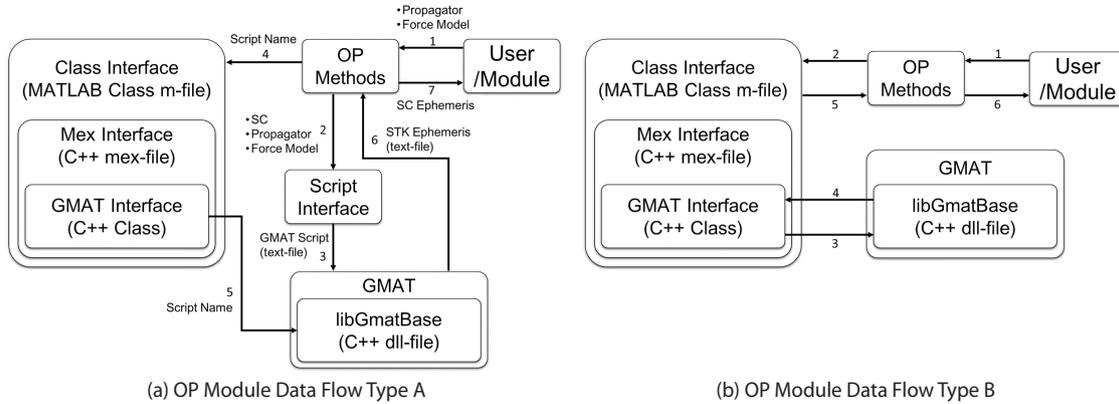
Fig. 2. OP module data flow diagram: (a) type A for orbit propagation and (b) type B for other operations.

class interface, MEX interface, GMAT interface, GMAT base library (libGmatBase.dll), and GMAT data files. Note that these components are either binaries or classes written in MATLAB or C++. Finally, there are four public classes accessible by any module: the air-drag model, the gravity potential model, the force model, and the propagator. These classes are used to deliver orbit propagation options, and are compatible with but not dependent on the GMAT. Using these public classes, the script interface class writes a GMAT script that gives an order to the GMAT regarding how to propagate the spacecraft trajectory.

Fig. 2 shows the two data flow diagrams of the OP module. Fig. 2(a) is the data flow diagram for orbit propagation, which shows that the class interface cannot directly access the GMAT base library (libGmatBase.dll) but contains the MEX interface, which can communicate with the GMAT base library. Note that for orbit propagation, most of the data communication is indirect and based on text file access, except for the name of the script, which is a string type data, and is directly delivered to the GMAT base library through the MEX interface. Moreover, Fig. 2(b) presents the data flows of the other operations such as time and coordinate system conversions and ephemeris generations of ground stations and celestial bodies. The specific data contents are omitted in the data flow diagram because they are dependent on the operation (or, method) being applied. Note that, in this

case, all data communication is direct and based on memory access so that type casting between MATLAB and GMAT data types is required. The GMAT uses an internal *Rvector* array type while the MEX interface uses its own *mxArray* type, where non-standard C++ type identifiers are denoted in italics. Thus, the MEX interface converts *Rvector* to *mxArray* and vice versa using the standard C++ type array.

4. EP MODULE

The EP module predicts astrodynamics-related events, and delivers information on the timing and type of event to the user or the OD module to aid the mission planning and design process. The highest-level data flow diagram is provided in Fig. 1(a). The EP module addresses various types of events such as orbital status, eclipses, ground station visibility, and solar communication outages. However, the current implementation of the EP module does not consider special relativistic light time delay and stellar aberration. The EP module was developed to support the KPLO and, in the Earth-Luna system, perturbation effects usually cause errors of less than a few seconds. Future extension of the EP module may include these perturbation effects for applications to other deep space missions beyond the Earth-Luna system.

The EP module consists of event functions, an event

location algorithm, a mesh-refinement algorithm, and public classes. The event functions are defined for different types of event in that when an event occurs, the event function value is equal to zero. For instance, Eq. (8) is an event function for solar communication outage. As a result, finding roots of the event function is equivalent to locating the events. The event location algorithm finds the location and type of events by solving the root-finding problem with the data provided (i.e., event function and ephemerides of spacecraft, ground stations, and celestial bodies). To find the roots of the event function, the event location algorithm utilizes the cubic Hermite spline and analytical roots of the cubic equation. The mesh-refinement algorithm estimates the quality of the event prediction solution and updates the mesh-points used in the root-finding so that the quality of the event prediction solution satisfies the user-defined tolerance. There are two public classes in the EP module: point-type event prediction and interval-type event prediction classes. These classes contain information on the location and type of events obtained by the event location algorithm.

4.1 Functionality Requirements

The current list of event prediction functionality requirements for the KPLO is presented in Table 3 (Song et al. 2016). Each functionality code (i.e., EPF-1) indicates a category of the functionality requirement. If necessary, a functionality code can be divided into multiple functionality sub-codes (i.e., EPF-1.1, EPF-1.2, and EPF-1.3) because an event may be determined by multiple geometrical configurations. For instance, ground station visibility is acquired only when the elevation of the spacecraft is higher than the cut-off angle of the ground station and the signal is not occulted by any celestial body. Although functionality codes appear fairly fixed, new functionality sub-codes can be added in the future. For instance, EPF-3, which is an orbital status event, is expected to have more minor functionality codes than at present because the KPLO's detailed mission requirements are still to be determined.

4.2 Event Location Process

The mathematical details of the event location process are provided here. The mesh-refinement algorithm controls the outer loop of the event prediction process while the event location algorithm controls the inner loop. The mesh-refinement algorithm controls the overall quality of the event prediction solution. The event location algorithm consists of two components: the cubic Hermite spline and the analytical root-finding algorithm for cubic equations. The approach taken here has merits in that it does not require any iterative process in root-finding. The cubic Hermite spline utilizes the first derivatives, and it has a better accuracy than the (natural) cubic spline, which does not use any derivatives. An error control scheme (for instance, mesh refinement) is not applied at the event location algorithm level but at the mesh-refinement level.

The flow chart for the event prediction process is presented in Fig. 3. The user provides the spacecraft ephemeris and initial mesh configuration for the time domain. With the given mesh points, the OP module is asked to produce the ephemerides of celestial bodies and ground stations. Based on this, the *event function* subroutine provides event function values and its first derivatives at mesh points. For each mesh interval, the *cubic Hermite spline* subroutine defines a third-degree polynomial specified for the Hermite form based on event function values and its first derivatives at the end points of the interval. For each cubic function defined in an interval, the *analytical root-finding* subroutine for cubic polynomials analytically determines all inside roots. By repeating root-finding for all intervals, the event location is completed. The mesh-refinement algorithm increases the time sampling rate by ten times, and compares the relative errors of the roots between two different mesh configurations. The mesh-refinement algorithm continues increasing the

Table 3. Event prediction functionality requirements for KPLO

Functionality Code	Functionality Sub-Code	Description
EPF-1		Predict eclipse by major planetary bodies in Earth, Luna, and trans-Lunar orbits
	EPF-1.1	Predict umbra Entry and Exit by ellipsoidal body in Earth, Luna, and trans-Lunar orbits
	EPF-1.2	Predict penumbra Entry and Exit by ellipsoidal body in Earth, Luna, and trans-Lunar orbits
	EPF-1.3	Predict antumbra entry and exit by ellipsoidal body in Earth, Luna, and trans-Lunar orbits
EPF-2		Predict solar outage in Earth, Luna, and trans-Lunar orbits
EPF-3		Predict orbital status in Earth, Luna, and trans-Lunar orbits
	EPF-3.1	Predict apsis passage in Earth, Luna, and trans-Lunar orbits
	EPF-3.2	Predict node crossing in Earth, Luna, and trans-Lunar orbits
EPF-4		Predict ground station visibility in Earth, Luna, and trans-Lunar orbits
	EPF-4.1	Predict elevation angle cut-off in Earth, Luna, and trans-Lunar orbits
	EPF-4.2	Predict communication interruption by celestial bodies in Luna orbit
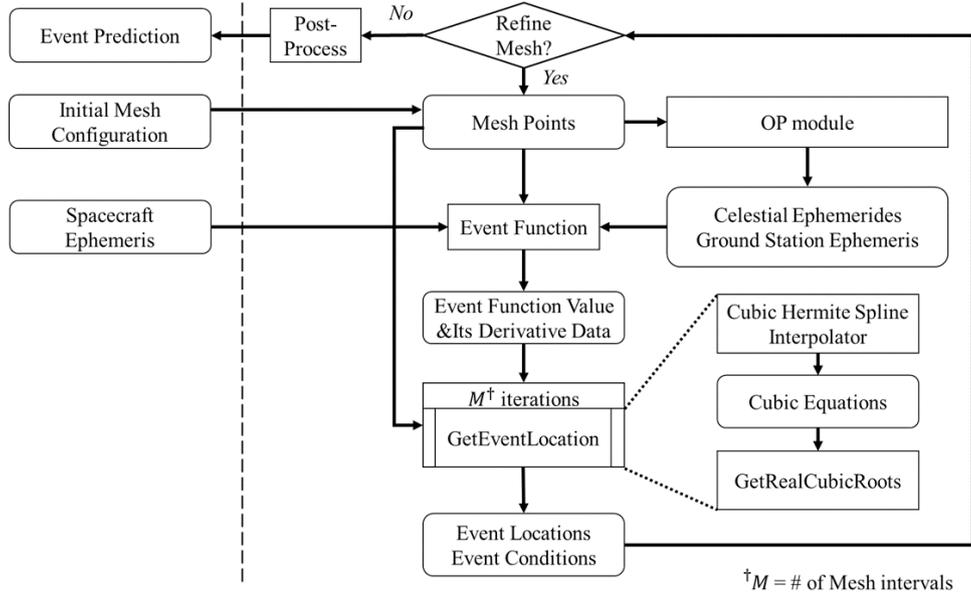
Fig. 3. Data flow chart for the event location process.

time sampling rate until all the relative errors satisfy the user-defined tolerance or the iteration counts reaches the user-defined maximum iteration constraint. As the end product, the locations of the events and the event conditions (e.g., whether it is the beginning or end of the event) are delivered to the user as the point-type event prediction or interval-type event prediction class.

The cubic Hermite spline defines a third-degree polynomial in Hermite form using the function value and its first derivative at the end points of an interval (Zill et al. 2011):

$$\hat{g}_{n,n+1}(t) = a_3(t-t_n)^3 + a_2(t-t_n)^2 + a_1(t-t_n) + a_0 \quad (5)$$
$$(t_n \leq t \leq t_{n+1})$$

where $\hat{g}_{n,n+1}(t)$ is the third-degree polynomial in Hermite form and t_n is n-th mesh point. The coefficients, presented in Eq. (5), are given as follows:

$$\begin{bmatrix} a_0 \\ a_1 \\ a_2 \\ a_3 \end{bmatrix} = \begin{bmatrix} 1 & 0 & 0 & 0 \\ 0 & 1 & 0 & 0 \\ 1 & h & h^2 & h^3 \\ 0 & 1 & 2h & 3h^2 \end{bmatrix} \begin{bmatrix} g_n \\ \dot{g}_n \\ g_{n+1} \\ \dot{g}_{n+1} \end{bmatrix} \quad (6)$$

where $h = t_{n+1} - t_n$, $g_n = g(t_n, \mathbf{X}(t_n))$ and $\dot{g}_n = \dot{g}(t_n, \mathbf{X}(t_n))$. Compared to the natural cubic spline, the cubic Hermite spline generally achieves a better interpolation accuracy using the first derivatives when constructing the cubic equation in an interval. The absolute accuracy, as opposed to the relative accuracy, of the cubic Hermite spline is affected by both the event function and mesh point configuration.

Although the analytical expressions of the roots of cubic equations are elementary, they are not presented here due to their complexity. Experience using the cubic Hermite spline and analytical roots indicates that even for real roots, the analytical roots obtained in the complex space can contain numerical noise in the complex component. They seem to be affected by the cubic Hermite spline and the MATLAB built-in algorithm for calculating the cubic roots in the complex space. However, for a typical mesh interval of 60 sec, the numerical noise in the complex component is less than $10^{-7}\sqrt{-1}$, which is infinitesimal with respect to event prediction for real mission applications. Thus, the EP module ignores numerical noise in the complex component of less than $10^{-7}\sqrt{-1}$ to effectively determine the real roots.

4.3 Example: Solar Outage Prediction

This subsection evaluates event prediction capability using a solar outage (or, solar interference) prediction example. Solar outage is a phenomenon whereby radio signals from a spacecraft are obscured by solar radiation. To prevent unexpected communication problems, it is necessary to predict the timing and duration of solar outage events for the entire mission duration. Note that the explanations for the example are rather brief because the objective here is not to justify the approach taken in the EP module but to give an idea how the EP module solves event prediction problems.

Here, a solar outage prediction simulation result is presented for a lunar orbiter. The outage angle defines when the outage occurs. If the angular separation between the spacecraft and the Sun is less than the outage angle, the signals from the spacecraft

are expected to be obscured by solar radiation. An empirical approximation formula for the outage angle θ_{SI} is adopted to predict solar outage, as follows (Vankka & Kestilä 2014):

$$\theta_{SI} = \frac{6\sqrt{BW}}{F_D D_A} + \theta_{Sun} \quad \text{in degree} \quad (7)$$

where $\theta_{Sun} = 0.25°$ is the apparent angular radius of the Sun, BW is the antenna beam width in decibels, F_D is the downlink frequency in GHz, and D_A is the antenna diameter in meters. Note that, typically, $BW\sim 3$ dB is assumed so that $6\sqrt{BW} \cong 10.4$. Using the hour angle α and the altitude angle δ measured at the ground station, an event function for the solar outage can be defined as follows:

$$g_{SI}(t, \mathbf{X}) = \cos(\theta_{SI}) - \cos(\Delta\alpha)\cos(\Delta\delta) \quad (8)$$

where $\Delta\alpha = \alpha_\odot - \alpha_{SC}$, $\Delta\delta = \delta_\odot - \delta_{SC}$, and the subscripts $\odot$ and SC represent the Sun and the spacecraft, respectively. From Eq. (8), the solar outage is expected to occur when $g_{SI}(t, \mathbf{X}) \leq 0$. Therefore, when $g_{SI}(t, \mathbf{X}) = 0$, the sign of $\dot{g}_{SI}(t, \mathbf{X})$ determines whether it is the beginning or end of the solar outage.

In the simulation, DSODS predicts the solar communication outage of a lunar orbiter observed by a nominal Daejeon station (36.38°N, 127.35°E, altitude = 102 m). This simulation begins at TAI 01 Sep 2035 10:00:00, and ends 23 hr later. The current simulation of solar outage is based on the total lunar eclipse, which will be observable by the Daejeon station at 02 Sep 2035 because, in usual conditions, solar outages are rare for lunar orbiters, and also a lunar orbiter can experience a solar outage when a solar eclipse is observable by the ground station. In this simulation, $\theta_{SI} \cong 0.35°$ is applied by setting $BW = 3.4$ dB, $F_D = 11.95$ GHz, and $D_A = 9$ m. The upper left and right figures in Fig. 4 present the spacecraft relative trajectory on the local celestial sphere of the Daejeon station with respect to the apparent Sun. The solar outage occurs when the spacecraft is located inside of the outage sphere. According to the figures, the solar outage occurs twice during the simulation. The lower left figure in Fig. 4 presents the solar outage event function for the entire duration, and the lower right figure in Fig. 4 presents this event function for 14-16 hr, where the solar outage occurs twice. These parts of Fig. 4 indicate that DSODS succeeded in locating all four real roots in the solar outage event function.

4.4 Validation and Verification Tests

To validate and verify DSODS's event prediction capabil-
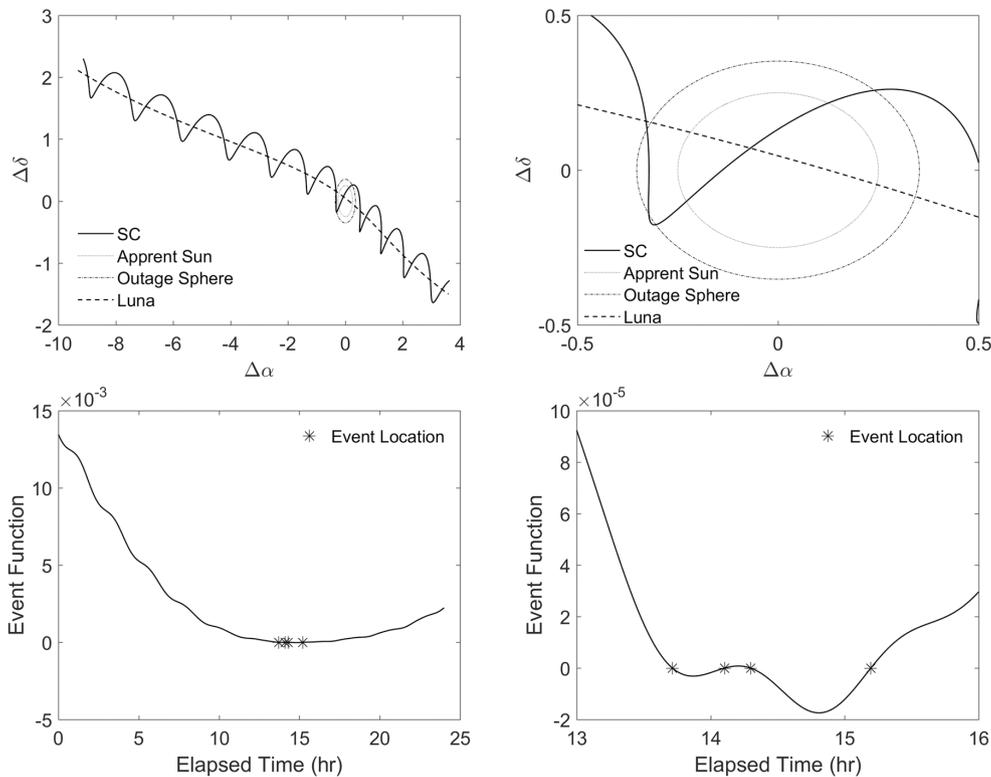
Fig. 4. Event prediction results: (upper left and right figures) showing the spacecraft relative trajectory on the celestial sphere on different scales, and (lower left and right figures) the event function values on difference scales.

Table 4. Event Prediction Validation and Verification Result Summary

Test Cases	Related Code	Central Body	Time Span	Possible Event Types	Number of Events Per Test	Truth Data Generator	Max Error (sec)
Eclipse	EPF-1.1 EPF-1.2 EPF-1.3	Earth	4 hr	Earth Penumbra Earth Umbra Luna Penumbra Luna Antumbra	13	SPICE	6.75E-3
Eclipse	EPF-1.1 EPF-1.2	Luna	12 hr	Luna Penumbra Luna Umbra	15	SPICE	1.35E-3
Eclipse	EPF-1.1 EPF-1.2	Mars	12,000 sec	Mars Penumbra Mars Umbra	5	SPICE	2.54E-2
Solar Outage	EPF-2	Earth	4 day	Solar Outage in C band	3	Cromack's Calculator	9.53
Solar Outage	EPF-2	Earth	4 day	Solar Outage in Ku band	3	Cromack's Calculator	8.28
Apsis Passage	EPF-3.1	Earth	1 day	Apogee Passage Perigee Passage	27	GMAT	2.52E-4
Apsis Passage	EPF-3.1	Luna	1 day	Aposelene Passage Periselene Passage	19	GMAT	2.73E-4
Node Crossing	EPF-3.2	Earth	1 day	Ascending Node Crossing Descending Node Crossing	26	GMAT	6.16E-6
Node Crossing	EPF-3.2	Luna	1 day	Ascending Node Crossing Descending Node Crossing	19	GMAT	4.05E-4
GS Visibility	EPF-4.1	Earth	1 day	Elevation Cut-Off	6	STK	3.10E-2
GS Visibility	EPF-4.1 EPF-4.2	Luna	2 day	Elevation Cut-Off Luna Occultation	10	STK, GMAT	2.57E-2

ities, eleven test cases were implemented according to the functionality requirements presented in Table 3, and corresponding test results are presented in Table 4. When DSODS was executed for event prediction under a typical desktop environment, each test case took up to a few tens of seconds. For most test cases, external truth data were provided by various sources including GMAT, STK, or SPICE, whose event prediction capabilities have been proved through a number of real mission applications. Also, for most functionality codes, there were at least two tests simulated in Earth and Luna orbits, except EPF-2, which relates to solar outage. No tests on trans-lunar orbits were included in the test cases because a trans-lunar orbit is essentially an Earth orbit in terms of its dynamic characteristics.

For the tests on EPF-1, which relates to an eclipse by an ellipsoidal body, there were three test cases simulated for Earth, Luna, and Mars because Mars is a more oblate body than Earth so a Mars orbit is a better testbed to check the effects of an ellipsoidal body. In addition, antumbra and umbra are mutually exclusive, while umbra is a more common event than antumbra. Thus, a carefully designed simulation was conducted to generate and test Luna antumbra prediction using an annular solar eclipse, which will be observed by ground observers on 26 Jan 2028 (GSFC 2017).

The test problem setting on the functionality code EPF-2 was different from the other cases in two aspects: first, only tests in Earth orbits were solved; and second, the truth data

were produced by a web calculator (Cromack Industries Inc. 2017) rather than flight-proven software such as SPICE or STK. The two differences arose because solar outages regularly occur for geostationary satellites, and most analyses were focused on satellites in geostationary orbits. As a result, the test cases on EFP-2 included two tests for C and Ku bands to test the dependency on the uplink frequency (see Eqs. (5)-(6)) instead of central bodies and orbits. It is suggested that the tests on solar outage prediction were less robust than the other functionality codes. However, DSODS's responsibility on solar outage prediction is limited to provide only an approximate geometrical estimation on solar outage rather than an accurate communication quality prediction, which requires radio engineering-based analysis on spacecraft and ground stations with a number of parameters (Vankka & Kestilä 2014). Therefore, applying less robust tests for solar outage prediction can be justified by limiting DSODS's responsibility to geometrical prediction rather than radio engineering-based communication quality prediction.

The KPLO does not yet have solid performance requirements on event prediction capabilities; therefore, the current verification results are preliminary and not confirmed. However, as shown in Table 4, most test cases showed a maximum error in the range of 10^{-2} sec compared to the truth data obtained by other software packages. DSODS's maximum error level agrees with the differences in the event predictions made by distinct software packages like STK, GMAT, and SPICE. For instance, the difference between Earth eclipse predictions made by SPICE

and STK are on the sub-second level. Therefore, considering that the responsibility of the EP module is to aid the mission planning and design process, a maximum error level of 10^{-2} sec is thought to be sufficient to satisfy KPLO's event prediction capability requirements. Moreover, the event prediction results on solar outages are different from those of a web calculator by less than ten seconds. To achieve the best matches, the following parameter values are used: $\theta_{Sun} = 0.5°$, $BW = 2.5$ dB, $F_{D,C-band} = 4.0$ GHz, and $F_{D,Ku-band} = 12.0$ GHz. Note that it is possible to reduce the differences between DSODS solar outage prediction and the external data by tuning related parameters. However, it does not seem critical because the responsibility of DSODS is to provide an approximate geometrical estimation on the occurrence of solar outages rather than an accurate link margin design and analysis.

5. SUMMARY AND CONCLUSIONS

DSODS has been developed to support the KPLO mission, and its development objective is to provide the following functionalities: orbit determination with DSN measurement models using the batch least squares estimation; DSN tracking data simulation; and event prediction to aid mission planning and design. To achieve the development objective, DSODS consists of one library and four modules: CUCL, OP, OD, DS, and EP, and uses the MATLAB object-oriented programming approach. The module-level data flow diagrams, presented in Section 2, explain how the modules interact with each other to perform orbit determination, measurement data simulation, and event prediction. To address some key concepts commonly used by all modules, the CUCL includes epoch time, coordinate system base, spacecraft, ground station base, and Hermite ephemeris classes. These classes are used in modular level interfaces, and play an important role in supporting various input and output interface specifications. Details of these classes are explained in Section 2.

To save time and effort on the development period, DSODS utilizes the GMAT as a third-party software for fundamental astrodynamics-related operations such as time and coordinate system conversions and high-fidelity orbit propagation in deep space. Although utilizing the GMAT affects the execution environment and limits the applicability of DSODS, all dependence on the GMAT is isolated in the OP module so that the GMAT can be replaced with other third-party software, if necessary.

Regarding the validation and verification of DSODS's event prediction capabilities, eleven test cases were implemented to cover all functionality requirements. Although the KPLO does

not yet have solid performance requirements, the achieved accuracy level of event prediction seems to be sufficient to support the KPLO for mission design and planning. As presented in Section 4, the event prediction results on most test cases showed a maximum error in the range of 10^{-2} sec, compared to the flight-proven mission analysis software packages such as GMAT, STK, and SPICE. Moreover, sub-second level differences in event predictions can be observed between them. Less accurate event prediction results were only obtained for solar outage prediction, with errors less than 10 sec obtained due to the uncertainty of related parameters in the simulation. However, such errors in solar outage prediction are not thought critical for real mission applications because DSODS is responsible for providing an approximate geometrical estimation of the occurrence of solar outages rather than an accurate link margin design and analysis on solar interference, which requires detailed radio engineering analyses.

ACKNOWLEDGMENTS

REFERENCES

Cappellari JO, Velez CE, Fuchs AJ, Mathematical theory of the Goddard trajectory determination system, NASA Goddard Space Flight Center, NASA-TM-X-71106 (1976).

Cromack Industries Inc., Satellite - Sun Outage Calculator [Internet], cited 2017 May 29, available from: http://www.cromack.com/satsun.html

D'Ortenzio MV, Bresina JL, Crocker AR, Elphic RC, Galal KF, et al., Operating LADEE: mission architecture, challenges, anomalies, and successes, in 2015 IEEE Aerospace Conference, Big Sky, MT, 7-14 Mar 2015.

GMAT, GMAT Mathematical Specification Document [Internet], 2017 May 29, available from: https://gmat.gsfc.nasa.gov/docs/GMATMathSpec.pdf

GSFC, Solar Eclipse Prediction [Internet], cited 2017 May 29, available from: https://eclipse.gsfc.nasa.gov/SEgoogle/SEgoogle2021.html

Hughes SP, Conway DJ, Parker J, Using the general mission analysis tool (GMAT), NASA Technical Report Server, GSFC-E-DAA-TN39043 (2017).

JPL, MONTE introduction [Internet], cited 2017 May 29, available

from: https://montepy.jpl.nasa.gov

Kim M, Kim Y, Lee E, Park SY, Kim YR, et al., Validation of DSN measurement model using Lunar Prospector tracking data, in KSAS 2017 Spring Conference, Samcheok, Republic of Korea, 19-22 Apr 2017a.

Kim Y, Kim M, Lee E, Park SY, Kim YR, et al., Performance validation of orbit determination software using Lunar Prospector tracking data, in KSAS 2017 Spring Conference, Samcheok, Republic of Korea, 19-22 Apr 2017b.

Lee E, Kim Y, Kim M, Park SY, Kim YR, et al., In/Out function of orbit determination software and overlap analysis of Lunar Prospector trajectory, in KSAS 2017 Spring Conference, Samcheok, Republic of Korea, 19-22 Apr 2017.

Moyer TD, Formulation for Observed and Computed Values of Deep Space Network Data Types for Navigation (John Wiley & Sons, Hoboken, 2005).

ODTBX (Orbit Determination Toolbox), Mean meteorological parameters [Internet], cited 2017 May 29, available from: https://sourceforge.net/projects/odtbx/

Parker JJK, Hughes SP, A general event location algorithm with applications to eclipse and station line-of-sight, in AAS/AIAA Astrodynamics Specialist Conference, Girdwood, AK, 31 Jul – 4 Aug 2011.

Song YJ, Lee D, Bae JH, Kim BY, et al., Preliminary Design of LUDOLP: the flight dynamics subsystem for the Korea pathfinder lunar orbiter mission, in 14th International Conference on Space Operations, Daejeon, Republic of Korea, 16-20 May 2016.

Thornton CL, Border JS, Radiometric Tracking Techniques for Deep-space Navigation (John Wiley & Sons, Hoboken, 2003).

Vankka J, Kestilä A, Sun outage calculator for geostationary orbit satellites, J. Eng. 26, 21-30 (2014).

Woodburn J, Seago JH, Orbit determination of satellites in lunar orbit using an optimal sequential filter, in 18th AAS/AIAA Space Flight Mechanics, Galveston, TX, 27-31 Jan 2008.

Zill DG, Wright WS, Cullen MR, Advanced Engineering Mathematics, 4th edition (Jones & Bartlett Learning, Sudbury, 2011).